AD-A130 044 PHASE CONJUGATE OPTICAL RESONATOR(U) HUGHES RESEARCH 1/1
LABS MALIBU CA R K JAIN APR 82 AFOSR-TR-83-0543
F49620-80-C-0041

UNCLASSIFIED F/G 20/6 NL

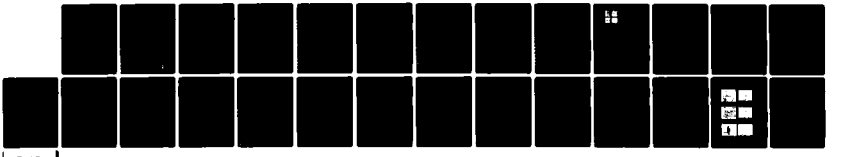

END
DATE FILMED
8-83
DTIC

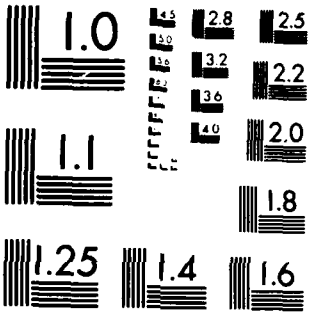

MICROCOPY RESOLUTION TEST CHART
NATIONAL BUREAU OF STANDARDS 1963-A

PHASE CONJUGATE OPTICAL RESONATOR

R.K. Jain

Hughes Research Laboratories
3011 Malibu Canyon Road
Malibu, CA 90265

April 1982

F49620-80-C-0041

Interim Technical Report

For Period 15 July 1981 through 14 March 1982

Sponsored By
AIR FORCE OFFICE OF SCIENTIFIC RESEARCH
Bolling AFB, D.C. 20332

UNCLASSIFIED

SECURITY CLASSIFICATION OF THIS PAGE (When Data Entered)

REPORT DOCUMENTATION PAGE	READ INSTRUCTIONS BEFORE COMPLETING FORM
1 REPORT NUMBER: AFOSR-TR- 83-0543	2 GOVT ACCESSION NO.: AD-A130044	3 RECIPIENT'S CATALOG NUMBER
4. TITLE (and Subtitle): PHASE CONJUGATE OPTICAL RESONATOR	5. TYPE OF REPORT & PERIOD COVERED: Interim Report, July 1981 - March 1982
	6 PERFORMING ORG. REPORT NUMBER
7. AUTHOR(s): R. K. Jain	8. CONTRACT OR GRANT NUMBER(s): F49620-80-C-0041
9. PERFORMING ORGANIZATION NAME AND ADDRESS: Hughes Research Laboratories, 3011 Malibu Canyon Road, Malibu, CA 90265	10 PROGRAM ELEMENT, PROJECT, TASK AREA & WORK UNIT NUMBERS: 61102F, 2301/A1
11. CONTROLLING OFFICE NAME AND ADDRESS: Air Force Office of Scientific Research, Bolling Air Force Base, DC 20332	12 REPORT DATE: April 1982
	13 NUMBER OF PAGES: 25
14 MONITORING AGENCY NAME & ADDRESS (if different from Controlling Office)	15 SECURITY CLASS (of this report): Unclassified
	15a DECLASSIFICATION DOWNGRADING SCHEDULE

16 DISTRIBUTION STATEMENT (of this Report)

Approved for public release; distribution unlimited.

17. DISTRIBUTION STATEMENT (of the abstract entered in Block 20, if different from Report)

18. SUPPLEMENTARY NOTES

19. KEY WORDS (Continue on reverse side if necessary and identify by block number)

Phase conjugation, Laser resonators, Optical resonators, Degenerate four-wave mixing, Phase conjugate mirror, Laser modes, Aberration correction

20 ABSTRACT (Continue on reverse side if necessary and identify by block number)

During this reporting period, a paper on the study of longitudinal modes and the aberration correction potential of a PCR based on a continuous-wave dye laser with a sodium phase conjugate mirror was published in Optics Letters as well as a paper on multiresonant behavior in nearly degenerate four-wave mixing in sodium. In addition, we report the

DD FORM 1 JAN 73 1473 EDITION OF 1 NOV 65 IS OBSOLETE

UNCLASSIFIED

SECURITY CLASSIFICATION OF THIS PAGE (When Data Entered)

UNCLASSIFIED

SECURITY CLASSIFICATION OF THIS PAGE(When Data Entered)

measurement of spatial and temporal properties of a PCR based on the photorefractive crystal $BaTiO_3$, and pumped with mW power levels from a He-Ne or a Kr^+ ion laser. In the absence of an intracavity aperture, the output beam is observed to be elongated in the plane of the crystal axis, via preferential self-defocussing of the beam due to the large anisotropy of the photorefractive effect in $BaTiO_3$. The resonator buildup time constants are found to be significantly larger than the time constants of the photorefractive response, particularly when the coherence length of the pump lasers are much smaller than the round-trip distance in the phase-conjugate resonator.

UNCLASSIFIED

SECURITY CLASSIFICATION OF THIS PAGE(When Data Entered)

PREFACE

This interim technical report was prepared by Hughes Research Laboratories under Air Force Office of Scientific Research Contract F49620-80-C-0041. The principal investigator is R.A. MacFarlane. R.K. Jain, G.J. Dunning, R.C. Lind and D.G. Steel performed the experimental work. Both C.R. Giuliano and R.L. Abrams provided continuous technical consultation throughout the contract. Theoretical assistance was provided by T.R. O'Meara and G.C. Valley under internal support by the company. Technical assistance was provided by J. Brown and J.P. Shuler.

We wish to thank H. Schlossberg from the Air Force Office of Scientific Research, the technical monitor, for his interest and support in this work.

PHASE CONJUGATE RESONATOR

This is the second interim technical report on a continuing program to study the properties of phase conjugate optical resonators. In particular, the objectives of this portion of the program are to demonstrate oscillation in a phase conjugate resonator (PCR), to examine its mode properties and to compare experiment with theory when possible. The unique property of phase conjugate mirrors to generate so-called time-reversed wavefronts has been demonstrated by workers at HRL and elsewhere. The use of this phenomenon to compensate for optical aberrations makes it a promising candidate for intracavity application.

The multipass character of laser oscillators greatly enhances the distortion potential of intracavity perturbations. In particular, the effect of laser medium index inhomogeneities resulting from flow variations, pump variations, or simply thermal effects can degrade the wavefront exiting from a laser to a larger extent than can a similar extracavity disturbance. Similarly, the effect of mirror misalignments is greatly accentuated compared to normal (extracavity) optical trains.

In principle, the resulting wavefront errors can be corrected either intracavity or extracavity. However, these internal errors lead to both amplitude distortions and vignetting of the output beams that are not easily compensated with extracavity systems. Further, the resulting intracavity errors may sometimes have a very high spatial frequency content. Since nonlinear conjugation and/or other nonlinear compensation offers excellent capability for correcting high spatial frequency distortion, as contrasted with conventional adaptive optics with deformable mirrors, it provides an important motivation for using such systems in intracavity compensation. In addition, a conjugate resonator offers the promise of recovering some of the energy that would be lost by diffraction in an ordinary resonator, resulting in improved energy extraction from the gain medium. Finally, the nonlinear approaches offer the ultimate promise of simplicity and low cost compared with deformable mirror systems.

In spite of the potential just discussed, there are many open questions concerning the application of nonlinear compensation in laser oscillators and the work performed on this program is aimed at answering these questions.

During this reporting period (July 1981 to March 1982), a paper on the study of longitudinal modes and the aberration correction potential of a PCR based on a continuous-wave dye laser with a sodium phase conjugate mirror was published in Optics Letters (Appendix A), as well as a paper on multi-resonant behavior in nearly degenerate four-wave mixing in sodium (Appendix B).

In addition, we report the measurement of spatial and temporal properties of a PCR based on the photorefractive crystal $BaTiO_3$, and pumped with mW power levels from a He-Ne or a Kr^+ ion laser. In the absence of an intra cavity aperture, the output beam is observed to be elongated in the plane of the crystal axis, via preferential self-defocussing of the beam due to the large anisotropy of the photorefractive effect in $BaTiO_3$. The resonator buildup time constants are found to be significantly larger than the time constants of the photorefractive response, particularly when the coherence length of the pump lasers are much smaller than the round-trip distance in the phase-conjugate resonator. The details of thi experimental investigation are described in a paper submitted for publication to Optics Letters. This paper is included as Appendix C.

APPENDIX A

Demonstration of the longitudinal modes and aberration-correction properties of a continuous-wave dye laser with a phase-conjugate mirror

R. C. Lind and D. G. Steel

Hughes Research Laboratories, Malibu, California 90265

Received July 20, 1981

We have experimentally demonstrated a cw dye laser incorporating a phase-conjugate mirror (PCM). The mirror was generated by using four-wave mixing in sodium. The unique bandwidth and pump–probe detuning properties of such a PCM permitted the first reported demonstration of the $c/4L$ spaced paired half-axial modes. In addition, the aberration correction ability is demonstrated.

The spatial and spectral properties of phase-conjugate mirrors (PCM's) generated by resonantly enhanced[1-3] degenerate four-wave mixing (DFWM) have been studied in detail and have been shown to possess unique optical properties. The capability of DFWM to generate complete phase reversal of an incoming probe wave permits aberration correction in an optical system. Similarly, studies of the frequency dependence of pump–probe detuning have resulted in the predictions of unexpected frequency dependence.[4-6] Hence the concept of incorporating a PCM as one of the mirrors in a laser resonator leads to interesting possibilities and has been the subject of numerous calculations.[7-10] These results have shown that such Fabry–Perot resonators have longitudinal- and transverse-mode properties distinct from those of conventional resonators. In addition there have been experimental reports of lasing action in phase-conjugate resonators (PCR's).[7,11] Aside from interesting physical behavior, resonators using a PCM are also expected to find application in laser systems characterized by highly aberrating turbulence. Given the dynamic behavior of turbulence, the application requires real-time aberration correction. Therefore, the PCM used in such a PCR needs to be characterized by a response time shorter than the characteristic time of turbulence.

It is the purpose of this Letter to present the initial results of an experimental study of the first reported cw PCR employing a gain medium and a real-time phase-conjugate mirror with the potential for high-speed aberration correction. The generalized PCR consists of a broadband homogeneously broadened cw gain medium, a regular mirror output coupler, and a PCM. The PCM is produced by two counterpropagating pump beams supplied by a separate laser. The beams are incident in a medium possessing a large third-order nonlinearity. In our case this medium is atomic sodium in the gas phase. Given typical cw dye-laser gain values of g_0L, we require a moderately efficient DFWM response to achieve the oscillation condition (given by $e^{2g_0L} = R_1^{-1}R_{PCM}^{-1}$, where R_1 is the reflectivity of the output coupler and R_{PCM} is the reflectivity of the PCM). The output is extracted from the regular mirror, and, in the presence of intracavity aberrations, it is this beam that will exhibit the transverse cavity mode.

Establishing a measurement of both the frequency and spatial properties of a PCR requires a cw or quasi-cw PCM and gain medium. The minimum time depends on several parameters, including the cavity length, the Fresnel number, and the cavity lifetime. To ensure steady-state modes we operate in a cw configuration made possible by the high-reflectivity cw PCM that we demonstrate below.

The PCM is generated by four-wave mixing in Na vapor. In order to achieve oscillation it was necessary that the reflectivities exceed ~40%, consistent with the net gain in the system. We have demonstrated greater-than-unity reflectivities, with typical operation being in the 80% region. To obtain these high reflectivities we use the geometry shown in Fig. 1. The counterpropagating pump is obtained by splitting the main beam into a forward and a backward pump. It is important to operate with separate pumps to avoid the extra pump absorption and thus the unbalanced pumps that occur in the more-standard technique of passing the forward pump through the conjugator and then retroreflecting this beam into the conjugator to generate the backward pump. The unbalanced pumps resulting from this configuration produce a decrease in the reflectivity resulting from a reduction in the nonlinear response. This effect is a characteristic of the saturating resonant nonlinearity that gives rise to DFWM. In the present case the pump beams were obtained from a Coherent Radiation 699-21 stabilized dye laser producing 1.2 W of single-line power. This beam was focused with a 1-m focal-length lens into the Na cell, which was a simple 1-cm-long side-arm cell. To achieve high reflectivities the Na pressure was adjusted near 10^{-3} Torr with high cw output of the dye laser required to bleach the Na vapor. In addition to these factors, with linearly polarized pumps it is necessary to maintain a small angle between the pump and the probe to maximize the reflectivity, where the probe path of course is the path over which the PCR will oscillate. This sensitivity to angle is shown in the paper of Nilsen and Yariv[4] and is a characteristic of an inhomo-

Reprinted from Optics Letters, Vol. 6, page 554, November, 1981

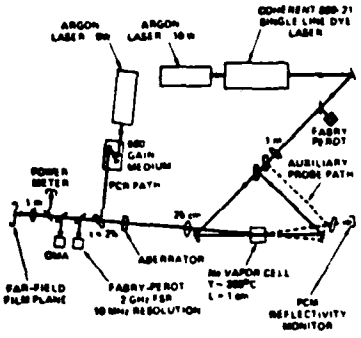

Fig. 1. Experimental configuration for a cw PCR. The PCM is produced by using DFWM in sodium vapor. The PCR gain medium is an argon-pumped dye laser using Rh6G dye.

geneously broadened medium such as Na vapor. For our experiments the angle was kept below ~0.5°. For alignment of the system the auxiliary probe path shown in Fig. 1 was used. The conjugate signal generated by this probe signal was used as a monitor on the reflectivity of the PCM as the PCR experiments progressed. It is important to note that these high reflectivities are only achieved by appropriately detuning the laser off line center of the D_2 transition[1] and by operation of the pump laser in a single longitudinal mode. The dependence of the reflectivity on the pump frequency (assuming degenerate operation) is quite complex because of the hyperfine splitting of the D_2 line ($\lambda = 589$ nm) into six dipole-allowed transitions. Optical pumping and the presence of many crossover resonances adds to the difficulty. Nevertheless, detailed studies of the PCM using the 699-21 dye laser have resulted in a fairly complete understanding of the various processes. Whereas earlier studies[2] of DFWM on this transition showed that the largest reflectivity ($R \sim 0.2\%$) was observed on the $3s^2\,S_{1/2}(F=2)$–$3p^2p_{3/2}(F=3)$ hyperfine transition, these new experiments showed that the largest reflectivities ($R \sim 150\%$) occurred near the $3s^2\,S_{1/2}(F=1)$–$3p^2\,p_{3/2}(F=0)$ transition.

Oscillation was achieved in the PCR along the path shown in Fig. 1. The gain medium consisted of a Coherent Radiation 590 dye laser with its output coupler removed and replaced by the 25-cm focal-length lens–PCM combination. The gain medium was pumped by a second argon laser, giving sufficient gain to reach threshold in the PCR. The regular mirror of the PCR was the 100% reflectivity mirror normally used with the 590. The path of the PCR in the 590 is as shown and is that normally associated with the 590 dye-laser configuration. The output of the PCR was obtained from that fraction of the energy coupled out of the beam splitter shown in Fig. 1 (~2%). The PCR output was monitored with an optical multichannel analyzer (OMA) and with a 10-MHz-resolution scanning Fabry–Perot étalon. The OMA indicated that the PCR output was at 5890 Å as expected, but when the PCM was replaced by a regular mirror (with reflectivity equal to that of the PCM) the laser oscillated near 5840 Å (at the peak of the gain for R6G).

The key feature that distinguishes a conventional laser resonator from the demonstrated PCR is the longitudinal-mode structure observed in the output frequency spectrum of the PCR. Whereas modes of an ordinary laser resonator are spaced by $c/2L$, the modes of the resonator incorporating a phase-conjugator mirror are spaced by approximately $c/4L$ and occur in pairs symmetrically spaced to the central frequency.[8] The central frequency always corresponds to the pump frequency of the PCM and is independent of the cavity length. In our experiments two distinct operating modes were observed: pure single longitudinal-mode output (without the use of any intracavity frequency-selecting elements) as shown in Fig. 2(a) and multimode structure consisting of the paired half-axial modes as shown in Fig. 2(b), with a frequency separation of $c/4L$ as expected.

To understand why these operating modes occur it is necessary to examine the pump–probe detuning characteristics of the nearly degenerate four-wave mixer geometry used to generate the PCM. We have established experimentally these characteristics at both high and low intensity and have found the behavior to be complicated. Our observations show basically that at high pump intensities the probe frequency at which the peak reflectivity of the PCM occurs need not coincide with the pump frequency. *Furthermore, the bandwidth of the PCM is also a function of the pump detuning from resonance.* To determine the effects of the PCM bandwidth on the PCR output, we compare this bandwidth with the $c/4L$ spacing of the PCR. In these experiments $c/4L \sim 40$ MHz; thus the first set of paired half-axial modes will occur with a total separation of 80 MHz. It was found that when the pump frequency was adjusted so that the peak reflectivity of the PCM oc-

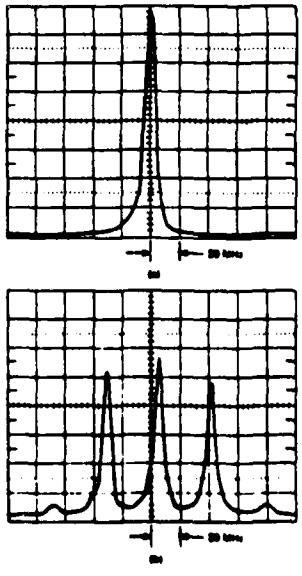

Fig. 2. Scanning Fabry–Perot signals of PCR output. (a) Single-mode output when the PCM bandwidth is less than $c/4L$. (b) Paired half-axial modes separated by $c/4L$ when the PCM bandwidth is of the order of 200 MHz.

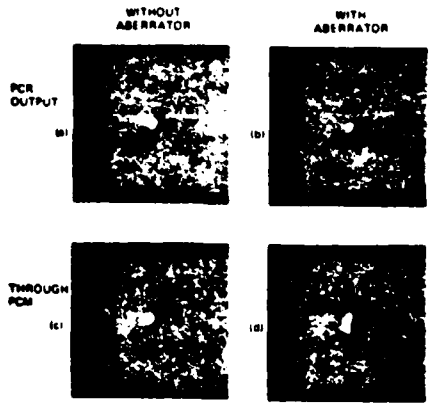

Fig. 3. Far-field photographs showing the aberration correction ability of the PCR. (a) and (b) Correction ability of the PCR output in the presence of an aberrator. (c) and (d) Output with the aberrator as observed through the PCM. As expected, (d) shows no correction, whereas (b) shows good correction.

curred for a probe frequency equal to the pump frequency, the PCR oscillated in a single longitudinal mode [Fig. 2(a)]. From the independent bandwidth measurements under these conditions it was found that the FWHM of the PCM filter was about 50 MHz, consistent with suppressing the modes that would oscillate at a separation of 80 MHz. However, when the pump frequency was repositioned so that the PCM bandwidth opened up to ~200 MHz, the PCR was observed to oscillate in several paired modes (consistent with the increased bandwidth) about the central frequency, which was degenerate to the pump frequency [Fig. 2(b)].

The peak output power observed from the PCR was measured and found to be about 1 mW. This is consistent with a calculation that takes into account the unique saturation characteristics of a PCR. In particular, in a conventional dye laser the saturation of the system is determined by the saturation intensity of the dye gain medium, which is of the order of 1 MW/cm^2. However, for a PCR oscillating with the geometry shown in Fig. 1 the saturation characteristics are determined by the PCM. That is, the maximum internal flux in the PCR can be no greater than the pump intensity used for the PCM. Therefore the saturation intensity of the PCR is the pump intensity of the PCM, which in this case is about 50 W/cm^2. If one assumes that the reflectivity of the conjugator saturates as $1/(1 + I/I_{sc})$, it is easy to show that the output power (assuming that mirror losses are negligible) is[13]

$$P_0 = (AI_{sc})\frac{(1-R_1)}{R_1 G_0}(R_1 R_{PCM} G_0^2 - 1)\ \mathrm{W},$$

where $G_0 = e^{gaL}$, I_{sc} is the conjugator saturation intensity, and A is the area of a resonator mode. We inferred G_0 from measurements made when the PCM was replaced by an ordinary mirror (coupled with standard expressions for output power from dye lasers). By using these numbers, a calculated value was obtained that was within an order of magnitude of that measured.

The spatial-mode properties of the resonator have not been analyzed; however, it was observed that the output beam had a central bright spot and was similar to the TEM_{00} mode.

Another unique feature of this PCR is its high-speed real-time correction capability. The correction speed is determined by the response time of the PCM, which for the present case is the radiative rate of Na, or about 16 nsec. Thus this PCR has a bandwidth-correction capability of ~100 MHz. The static aberration correction was demonstrated by using a fixed aberrator. A 10× diffraction-limited aberrator was inserted into the PCR cavity. The position of the aberrator with respect to the lens was such that the aberrator was imaged into the PCM (see Fig. 1). By using this technique it was possible to insert the aberrator into the cavity and move it without significantly affecting the PCR output. However, when the PCM was replaced with an ordinary mirror, no lasing action was observed until the aberrator was removed. Figure 3 shows the aberration-correction ability of the PCR. Figures 3(a) and 3(b) show the PCR output through the 2% output coupler, both without and with the aberrator, showing aberration correction. Figures 3(c) and 3(d) show the PCR beam that is transmitted through the PCM, without and with the aberrator, demonstrating, as expected, that no aberration correction is obtained on the beam transmitted through the PCM. (The aberrator is only single passed when the beam is observed at this position; see Fig. 1, dashed line.)

We would like to acknowledge the contributions to the PCR theory made by J. F. Lam, the development of the output-power expression by T. R. O'Meara, and numerous technical discussions with C. R. Giuliano and R. L. Abrams. This work was supported in part by the U.S. Air Force Office of Scientific Research under contract no. F49620-80-C-0041.

References

1. R. L. Abrams and R. C. Lind, Opt. Lett. 2, 94 (1978); 3, 205 (1978).
2. P. F. Liao, D. M. Bloom, and N. P. Economou, Appl. Phys. Lett. 32, 813 (1978).
3. R. C. Lind, D. G. Steel, J. F. Lam, R. K. Jain, and R. A. McFarlane, J. Opt. Soc. Am. 70, 599 (1980).
4. J. Nilsen and A. Yariv, J. Opt. Soc. Am. 69, 143 (1979); 71, 180 (1981).
5. T. Fu and M. Sargent III, Opt. Lett. 4, 361 (1979).
6. D. J. Harter and R. W. Boyd, IEEE J. Quantum Electron. QE-16, 1126 (1980).
7. J. AuYeung, D. Fekete, D. M. Pepper, and A. Yariv, IEEE J. Quantum Electron. QE-15, 1180 (1979).
8. P. A. Belanger, A. Hardy, and A. E. Siegman, Appl. Opt. 19, 479, 602 (1980).
9. I. M. Bel'dyugin and E. M. Zemskov, Sov. J. Quantum Electron. 9, 1198 (1979).
10. J. F. Lam and W. P. Brown, Opt. Lett. 5, 61 (1980).
11. J. Feinberg and R. W. Hellwarth, Opt. Lett. 5, 519 (1980).
12. D. G. Steel and R. C. Lind, Opt. Lett. 6 (to be published, December 1981).
13. This derivation assumed a saturation that is due to bleaching. If instead we assume saturation arising from pump depletion resulting from large R_{PCM}, we obtain the formula above but multiplied by $G_0^2 R_1$.

APPENDIX B

Multiresonant behavior in nearly degenerate four-wave mixing: the ac Stark effect

D. G. Steel and R. C. Lind

Hughes Research Laboratories, 3011 Malibu Canyon Road, Malibu, California 90265

Received August 14, 1981

We have experimentally studied the effects of pump–probe detuning in nearly degenerate four-wave mixing. The data show multiresonant behavior as a function of the pump-probe detuning at both low and high intensities. At low intensities, the structure is the result of Doppler motion. At high intensities, five-peak structure is observed and is explained by the standing-wave modulation of the ac Stark splitting of the atomic levels.

The successful application of resonantly enhanced degenerate four-wave mixing (FWM) to phase conjugation has resulted in several theoretical investigations of nearly degenerate FWM.[1-3] In this case the nonlinear response is evaluated when the frequency of the input probe is different from the frequency of the two pumps. This Letter presents the experimentally determined dependence of the resultant signal reflectivity as a function of pump–probe detuning in the limit of the weak pumps ($I_{\text{pump}} \ll I_{SAT}$) and strong pumps ($I_{\text{pump}} \gg I_{\text{SAT}}$).

To review the problem we consider a FWM geometry with the simple Doppler-broadened two-level atomic system shown in Fig. 1. We consider the case of two counterpropagating pumps E_f and E_b at frequency ω_1. The probe E_p is nearly collinear with the forward pump at frequency ω_2. The two-level system is resonant at frequency ω_0, and we assume that the pumps are detuned from resonance by $\omega_1 = \omega_0 + \Delta$ and that the probe is detuned from the pumps such that $\omega_2 = \omega_1 + \delta$. Phase matching shows that the resultant signal is counterpropagating to the probe and has a frequency given by $\omega_s = \omega_1 - \delta$.

The Doppler-broadened-system problem has been solved only in the limit of low-intensity pumps by using third-order perturbation theory.[1] For a given pump detuning from resonance, Δ, it is possible to determine the resonance condition for the pump–probe detuning, δ. The resonances are given by $\delta = 0 (\omega_2 = \omega_0 + \Delta)$ and $\delta = 2\Delta (\omega_2 = \omega_0 + 3\Delta)$. Physically the origin of the first resonance arises when the detuning between the two beams is less than the linewidth, enabling both the forward pump and the probe to interact simultaneously with the same group of atoms to produce a spatial modulation of the population from which the backward pump can scatter. The physical origin of the second resonance is somewhat more subtle, arising from a combination of Doppler effects. The forward pump, ω_1 detuned from resonance by Δ, is Doppler shifted into resonance for a particular velocity group v. The resonance observed in tuning the probe to $\delta = 2\Delta$ occurs at a frequency at which, in the rest frame of the atom, the atom sees the Doppler-shifted probe and the backward pump at the same frequency.

The pump–probe detuning problem has also been examined in the presence of arbitrarily strong pump fields in homogeneously broadened Doppler-free media. A steady-state solution to the quantum-mechanical transport equation has been found that is valid to all orders in the pump field and to first order in the probe and signal.[2,3] The qualitative solution to this problem may be anticipated by recalling the behavior of a two-level atom subject to a strong field at frequency ω_1 tuned near resonance at ω_0. The population will undergo strong oscillation between the two levels at an angular frequency given by the generalized Rabi frequency $\Omega' = [(\omega_1 - \omega_0)^2 + \Omega^2]^{1/2}$, where $\Omega = \mu E/\hbar$, μ is the transition dipole moment, and E is the electric field. This effect can be viewed as a splitting of each level into two levels separated by an energy $\hbar\Omega'$ and is known as the ac Stark effect. Hence one would expect such a system to be characterized by three resonances at frequencies $\delta = 0$ and $\delta = \pm\Omega'$. However, in nearly degenerate FWM the presence of strong counterpropagating pumps slightly complicates this expectation. The simultaneous action of both pumps produces a standing-wave modulation of the net electric field. Hence the Stark splitting of the levels is also spatially modulated, producing a macroscopic polarization with resonances anticipated by the presence of high-intensity fields and low-intensity fields. By using perturbation theory in stationary media, one can show that, in the presence of low-intensity pumps, pump–probe detuning resonances occur at $\delta = 0$ and $\delta = \pm\Delta$. Hence a total of *five* reso-

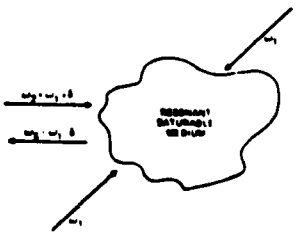

Fig. 1. Geometry for nearly degenerate FWM. The pumps are at frequency ω_1, but the probe is shifted by an amount δ.

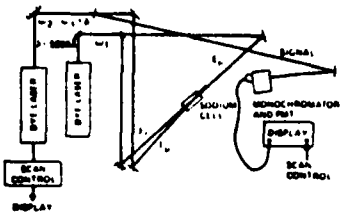

Fig. 2. Experimental layout for studying nearly degenerate FWM.

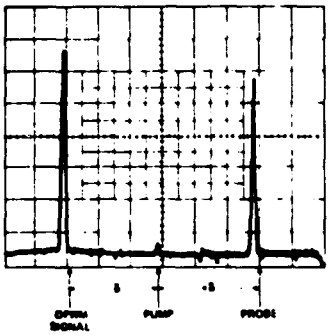

Fig. 3. Scanning Fabry–Perot signal showing the frequency shift of the signal wave ($-\delta$) with respect to the frequency shift of the input probe (δ) demonstrating that, because of phase matching, $\omega_1 + \omega_1 - \omega_2 - \omega_s = 0$.

nances is expected.[3] The ability to observe the low-intensity resonances in Doppler-broadened media might be expected only if the power broadening exceeded the pump detuning Δ.

The experimental study of nearly degenerate four-wave mixing was performed by using the experimental configuration shown in Fig. 2. A similar configuration was used by Nilson *et al.*[4] to demonstrate the narrow-band filter properties of FWM. The laser sources for the pumps (ω_1) and probe (ω_2) were two stabilized Coherent Radiation Model 699-21 tunable dye lasers with linewidths of the order of 1 MHz. The resonant atomic medium was sodium, and the lasers were tuned near the D_2 line (5890 Å). Because of the half-integral spin of the nucleus, the spectroscopy of the D_2 line is complex, with six allowed dipole transitions. Optical pumping plays an important role in the precise interpretation of any experiment involving sodium. However, if linearly polarized light is used, the effects are minimized by working on the strongest dipole transition, the $3s\ ^2S_{1/2}(F = 2)$–$3p\ ^2P_{3/2}(F = 3)$ transition characterized by a saturation intensity of the order of 6 mW/cm^2. The angle between the pump and the probe was minimized (<0.5°) for maximum reflectivity, defined as the ratio of the signal power to the input probe power. In all cases the probe intensity was kept well below the pump intensity. The absorption length product ($\alpha_0 l$) was kept at the order of 1.

The first measurement was a direct observation of the frequency phase-matching requirements. In general, $\omega_f + \omega_b - \omega_p - \omega_s = 0$. Therefore, since $\omega_f = \omega_b = \omega_1$ and $\omega_p = \omega_2 = \omega_1 + \delta$, we expect that $\omega_s = \omega_1 - \delta$. The verification of such behavior is critical for the occurrence of the paired half-axial modes predicted and observed in a laser resonator incorporating a phase-conjugate mirror.[5] Figure 3 shows a scanning Fabry–Perot trace of the signal obtained when the probe is detuned from the pumps. The figure also shows the probe frequency. As expected, the signal was displaced from the pump frequency an amount $-\delta$ when the probe was detuned an amount $+\delta$ from the pump. No additional structure was observed at either low or high pump intensities.

The experimentally measured dependence of reflectivity as a function of pump–probe detuning (δ) was taken at low pump intensity ($I \lesssim I_{SAT}$) for various pump detunings from the atomic resonance (Δ). Figure 4 shows the evolution of the resonant structure for various Δ as a function of probe frequency. As anticipated above, when $\Delta = 0$, there is a single strong resonance. However, as Δ is increased, two resonances form at $\delta = 0$ ($\omega_2 - \omega_0 = \Delta$) and $\delta = 2\Delta$($\omega_2 - \omega_0 = 3\Delta$). The bandwidth of the central resonance is determined by the longitudinal relaxation rate. For a two-lev problem with the lower state being the ground state. rate is given by the A coefficient. Hence the b width is twice as large as the atomic linewidth. Ph ly this rate is determined by how fast the popula (rather than the induced optical coherence) can re to the time-dependent optical field oscillating at (in the rotating-wave approximation). The ch eristic time for population dynamics (diagonal density matrix

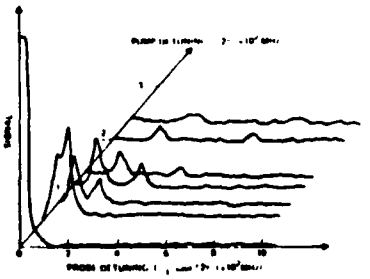

Fig. 4. Experimental demonstration of multiresonant behavior of nearly degenerate FWM for low pump intensity. The frequency shifts occur at $\delta = \Delta$ and $\delta = 2\Delta$, as expected for inhomogeneously broadened material.

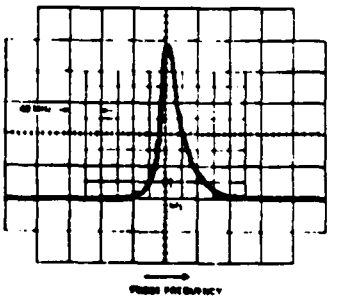

Fig. 5. The measured bandwidth of the pump–probe detuning response at low pump intensity. The width is determined by the longitudinal relaxation rate T_1^{-1}.

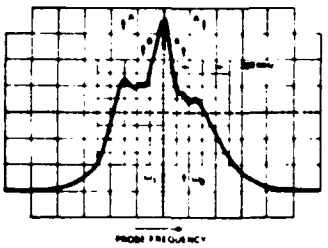

Fig. 6. The pump–probe detuning response as measured at high pump intensity. Five resonances are observed. The central resonance occurs at $\delta = 0$. The two structures designated B occur at $\delta = \pm\Delta$. The two structures designated A are due to the ac Stark splitting of the atomic levels and occur at $\delta = \pm\Omega'$.

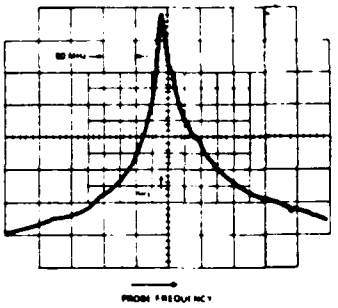

Fig. 7. The bandwidth of the pump–probe detuning signal under high-reflectivity conditions ($R \simeq 150\%$, $\alpha l \simeq 30$).

elements) is determined by the longitudinal relaxation time T_1 as opposed to the transverse relaxation time T_2 characteristic of optical coherences (off-diagonal density matrix elements). Figure 5 shows that the measured bandwidth is 25 MHz, in good agreement with the expected value of 20 MHz.

As expected at high intensities, the pump–probe detuning dependence is considerably more complicated. The interaction is further complicated in sodium by atomic motion and hyperfine structure. Nevertheless, by appropriate choices for the pump detuning Δ and pump intensity I it was possible to verify qualitatively the above predictions of multiresonant behavior. The observed five-peak behavior predicted by Harter and Boyd is shown in Fig. 6. The pump intensity was 23 W/cm^2, corresponding to $\Omega = 365$ MHz. The pump detuning was $\Delta = 210$ MHz, giving a generalized Rabi frequency of $\Omega' = 421$ MHz. As Fig. 6 shows, the location of the sidebands (structure A) agrees excellently with Ω'. Structure B is the resonance occurring at $\delta = \pm\Delta$. The dependence of the measured Ω' on the pump electric field is expected to be complicated because of velocity effects in the presence of the electric-field standing wave. However, our measurements show that, over a range of $0.1 < E < 0.45$ statvolt/cm, the measured Ω' corresponds to the calculated value. Whereas the origin of the resonant behavior appears to be anticipated by the analysis, a quantitative comparison between existing theory and experiment is not possible because of complicating effects that are due to velocity.

Not easily predicted or understood is the dip occurring at $\delta = 0 (\omega_2 = \omega_1)$. This structure has been observed to be very narrow (~30 MHz). Such an effect has been predicted to arise from a constructive interference arising between the probe and signal at $\delta \neq 0$. Such an explanation is not easily adapted to our data since this microstructure is a dip for $\Delta < 0$ and a spike for $\Delta > 0$ on the $3s^2\,S_{1/2}(F = 2)$–$3p^2\,P_{3/2}(F = 3)$ transition. Further, for transitions out of the $F = 1$ ground state, it is a dip for $\Delta > 0$ and a spike for $\Delta < 0$. Additional studies are in progress.

The net bandwidth in Fig. 6 is given by $2\Omega'$. However, as the absorption length product is increased, the bandwidth is observed to narrow significantly, and secondary resonances are not observed. This is so because the probe and signal are strongly absorbed as the detuning δ exceeds the frequency width of the hole burned by the strong saturating pumps. Furthermore, at high $\alpha_0 l$, the phase matching is no longer perfect because of a finite dispersion. However, under these conditions the reflectivity is over 150% on the $3s^2\,S_{1/2}(F = 1)$–$3p^2\,P_{3/2}(F = 0)$ transitions. An example of such a bandwidth is shown in Fig. 7.

In conclusion, we have experimentally observed the detailed and complex frequency structure associated with pump–probe detuning in nearly degenerate FWM. The understanding of such behavior, especially at high intensity, has been demonstrated to be critical for building a laser incorporating a phase-conjugate mirror. Furthermore, such interactions have been suggested for tunable narrow-band optical filters, and these experiments demonstrate how that bandwidth may be controlled.

The authors wish to acknowledge helpful discussions with R. A. McFarlane and J. F. Lam of Hughes Research Laboratories and R. Boyd and D. Harter of the University of Rochester. This work was supported in part by U.S. Air Force Office of Scientific Research contract no. F49620-C-0041.

References

1. J. Nilsen and A. Yariv, J. Opt. Soc. Am. 71, 180 (1981).
2. T. Fu and M. Sargent III, Opt. Lett. 4, 366 (1979).
3. D. J. Harter and R. W. Boyd, IEEE J. Quantum Electron. QE-16, 1126 (1980).
4. J. Nilsen, N. S. Gluck, and A. Yariv, Opt. Lett. 6, 380 (1981).
5. R. C. Lind and D. G. Steel, Opt. Lett. 12, (1981).

APPENDIX C

SPATIAL AND TEMPORAL PROPERTIES OF A CW PHASE-CONJUGATE RESONATOR BASED ON THE PHOTOREFRACTIVE CRYSTAL $BaTiO_3$

by

R. K. Jain and G. J. Dunning

Hughes Research Laboratories
3011 Malibu Canyon Road
Malibu, California 90265

ABSTRACT

We report measurements on spatial and temporal properties of a cw phase-conjugate resonator based on the photorefractive crystal $BaTiO_3$ and pumped with mW power levels from a He-Ne or a Kr^+ ion laser. In the absence of an intracavity aperture, the output beam is observed to be elongated in the direction of the crystal axis, via preferential self-defocussing of the beam due to the large anisotropy of the photorefractive effect in $BaTiO_3$. The resonator buildup time constants are found to be significantly larger than the time constants of the photorefractive response, particularly when the coherence length of the pump laser is much smaller than the round trip distance in the phase-conjugate resonator.

SPATIAL AND TEMPORAL PROPERTIES OF A CW PHASE-CONJUGATE RESONATOR BASED ON THE PHOTOREFRACTIVE CRYSTAL $BaTiO_3$

by

R. K. Jain and G. J. Dunning

Hughes Research Laboratories
3011 Malibu Canyon Road
Malibu, California 90265

Phase-conjugate mirrors based on degenerate four-wave mixing have been used recently to demonstrate the operation of cw phase-conjugate resonators, and to study their longitudinal modes and aberration correction properties.[1-3] Of particular interest for this application are the extremely high cw reflectivities[1] that are obtainable from phase conjugate mirrors based on photorefractive crystals such as barium titanate and barium strontium niobate[4,5], even with the use of relatively low pump powers. These high reflectivities are directly attributable to the magnitude of the photorefractive effect in these crystals, caused by the anomolously large values of appropriate electro-optic coefficients in these crystals ($r_{42} = 820 \times 10^{-12}$ mV^{-1} in $BaTiO_3$). It is well known[4-7] that the anisotropy of these electro-optic coefficients ($r_{13} = 8 \times 10^{-12}$ mV^{-1}, and $r_{33} = 23 \times 10^{-12}$ mV^{-1} for $BaTiO_3$) also causes large asymmetric self-defocussing of beams propagating through these crystals. In the present letter, we demonstrate experimentally the consequences of this intracavity self defocussing on the transverse modes of a $BaTiO_3$ based phase conjugate resonator (PCR), when no intracavity apertures are used. The effect of severe intracavity phase aberrators on the transverse mode profile is also studied. In addition, we report data on typical buildup times for steady state oscillation in such resonators, for cases when the

coherence length of the pump radiation is either much larger than or much smaller than the round trip distance in the phase conjugate resonator.

Figure 1 shows the experimental arrangement used for our degenerate four-wave mixing (DFWM) and PCR studies. BS1, BS2, and BS3 are 2%R, 18%R, and 66%R beamsplitters respectively, used to generate the three input waves for the DFWM experiments. These are designated by p, f, and b corresponding to the probe, forward pump and backward pump waves in the usual DFWM nomenclature[2], which correspond to the image, reference, and readout beams in the nomenclature of holography[1]. We will designate the corresponding beam powers and intensities by P_i and I_i respectively, where i = p,f, or b. ND represents variable neutral density filters that were used to attentuate the probe beam, and BB, M3, Ab, and L2 represent a beam blocker, partially transmitting mirror, aberrator and 5 cm focal length lens that were inserted only for PCR studies. The lens L2 allows focussing of all the light scattered by the aberrator into the pump volume determined by the overlap of the backward and forward pump waves; this not only improves the efficiency of the interaction, but is also essential for proper phase conjugation and aberration correction of this wave. The focal length of lens L1 was 100 cm; the path lengths of all three waves from this lens to the $BaTiO_3$ crystal was 110 cm $\pm$ 1 cm; the less than 2 cm path length difference was much smaller than the coherence length l_c of any of the lasers used in these experiments.

Experiments were performed using either a 15 mW multi-longitudinal mode TEM_{00} He-Ne laser output at 6328Å (ℓ_c ~20 cm), or using ~100 mW of multi-longitudinal mode or single longitudinal mode TEM_{00} power at 6471Å from a Kr^+ ion laser. A Faraday isolator was inserted between the experimental configuration of Fig. 1(a) and the pump laser to avoid instabilities associated with the inevitable retroreflection of beams from the experimental

configuration to the pump laser; this isolator was found to be crucial for well-characterized single longitudinal mode pumping of the PCR (and of the DFWM interaction). With multimode operation, the data corresponding to both the 6328Å and 6471Å experiments was very similar, except for the increased speed[1,3] at the higher 6471Å powers. For the data reported here, all of the beams were p-polarized, and the external angle θ (see Fig. 1(b)), between the probe and forward pump beams was maintained to be between 20 and 25 degrees. The 5 mm x 5 mm x 5 mm piece of single domain crystal $BaTiO_3$ was poled[8,9] by us just prior to these experiments, and was placed in a high refractive index (1.57) fluid, with an angular orientation (see Figure 1(b)) similar to that of Ref. 1

Using the above configuration, with backward pump-to-forward pump (I_b/I_f) and forward pump-to-probe (I_f/I_p) intensity ratios of between 4 to 1 and 10 to 1, phase conjugate reflectivities of over 200% were observed over a wide range of pump powers (from P_b ~5 mW to ~100 mW i.e. I_b ~5 W/cm^2 to ~100 W/cm^2) for both single longitudinal mode and multimode laser operation. For PCR operation, it is critical that the probe beam retraces its path exactly, which imposes a severe constraint on the relative angular alignment of the two pump beams. The angular fidelity of the phase conjugate return was checked with the use of a small variable aperture in the path of the probe beam. To obtain PCR operation, this aperture was removed, the probe beam was blocked (by BB in Fig. 1), and a partially transmitting mirror M3 (T=2% to T=40%) was oriented perpendicular to the path of the original probe beam. Oscillation of the PCR was then observed to occur with a relatively slow buildup time; we will first discuss the mode structure of the steady-state oscillation.

Figure 2 depicts far field photographs and transverse mode profiles of the output of such a "$BaTiO_3$ PCR," when pumped by single longitudinal mode

TEM_{00} radiation from a Kr^+ ion laser. All of these photographs were taken in the direction of M3, as indicated by the location of the video camera in Fig. 1. For these experiments, P_f = 0.75 mW and P_b = 3.5 mW, and an output coupler (M3) with T=7% was used. Figure 2(a) and 2(b) correspond to the case with no intracavity aperture or aberrator. It is observed that the "natural" transverse modes of such a resonator shows a distinct elongation (~4 to 1) in one direction. The elongation is in the plane defined by the input beams and the crystal axis, and is in qualitative agreement with the dominant beam coupling or beam defocussing in this direction due to the anisotropy of the photorefractive effect,[4-7] and the value of the numerical aperture (or acceptance angle) of lens L2. No attempts were made to model such transverse mode behaviour theoretically. Aperturing the beam results in a more circular spot, but with significant loss of output power,[10] as expected from spatial selection of the PCR transverse mode from the laterally elongated pump-probe overlap region in $BaTiO_3$.[6,7] The transverse mode profile of Figure 2(b) is along the direction of the horizontal cursor (white line) of Figure 2(a). The homogeneity of the beam profile was also observed to vary slowly with time (on a time scale of several seconds), and the slight dip in the oscilloscope photograph of Figure 2(b) is not a characteristic of the mode structure. Figs. 2(c) and 2(d) show far field photographs of the beam and the transverse mode profile when a severe aberrator is placed inside the cavity. The attenuation of the camera was reduced by an ND of 0.6, indicating a reduction in the beam intensity by approximately a factor of 3 due to the insertion loss of the aberrator. The relatively small change in the overall beam profile is indicative of excellent aberration correction, and is in strong contrast with the irregular mode patterns in the transverse mode data of Ref. 1. We do not understand the exact reasons for this discrepancy; however we did observe similar irregular mode patterns when we used

multi-longitudinal mode radiation for pumping the PCR. Figures 2(e) and (f) characterize the aberrator and were obtained by unblocking the probe beam, blocking the two pumps, and inserting a 100% retroreflector next to the aberrator (between the aberrator and lens L2), so that these pictures characterize the far-field pattern obtained after double passing the aberrator. Care was taken to ensure that the spatial region of the aberrator that was sampled by the probe beam was identical to the one for which the data of Fig. 2(c) and 2(d) were taken. We note that the mode profile of Figure 2(f) shows the shortcomings in the rendition of the intensity profile by merely a single-exposure photographic observation[1,2] (such as Fig. 2(e)), due to the lack of linearity of most photographic recording materials.

Additional experiments were performed to confirm that the observed output was indeed a PCR oscillation, and not merely due to self-sustained beam coupling effects[11,12] initiated by gratings that may have been written into the crystal at an earlier time. This included observations of the decay and buildup of the PCR oscillation with the blocking of the output coupler M3, and the observation that the PCR oscillation "tracked" small angular adjustments of this mirror in both the horizontal and the vertical planes. At pump power levels corresponding to a few mW (beam area ~0.1 mm^2, i.e. pump power densities of a few Watts/cm^2), the typical buildup and decay times of the PCR were observed to be of the order of several seconds (~25 seconds for I_f = 1.2 W/cm^2, I_b = 5.6 W/cm^2), and were comparable to the measured response times of the $BaTiO_3$ crystal at these power densities.

When the $BaTiO_3$ crystal was pumped with a multi-longitudinal mode laser (He-Ne or Kr^+), such that its coherence length (ℓ_c ~8 cm for Kr^+) was much shorter than the round trip distance (~30 cm) in the PCR, buildup oscillation was still observed to occur in the PCR cavity. However, this oscillation was

extremely sluggish, with buildup and decay times that were nearly two orders of orders of magnitude larger than the corresponding values of material reponse times. Because of the lack of phase coherence between the oscillating beams and the pump beams, it is surprising that any PCR buildup occurs at all, and the observed buildup is perhaps itself a measure of this coherence. However, as indicated earlier, the observed transverse mode profile was of much more irregular character than that shown in Figure 2. Nevertheless, negligible degradation in the far field mode pattern was observed even when very severe aberrators were introduced into the cavity.

It is conceivable that the coherence constraints imposed for multimode pumping could be satisfied much better if the $BaTiO_3$ crystal were moved one resonator length L away in the direction of the backward beam, so that the readout beam b arrives at a time 2L/c earlier than its precisely coherent counterpart in the reference beam f. Then, the scatter of the readout beam b by the dominant steady-state (f-p) grating would result in a wave that returns often one round trip (i.e. 2L/c) delay in the PCR, as an image beam p that is coherent with f, the other writing beam. A steady state self-consistent solution may thus be possible, in which the dominant intracavity flux ("p") in the PCR closely satisfies the requirements of coherence with respect to the forward pump f. We have not as yet attempted any experiments or the precise modeling of such a PCR configuration.

With the use of high output couplings, net efficiencies of over 25% were easily obtained in the PCR output power relative to the sum of the input powers, despite the large intracavity losses caused by spurious reflections. In the case of large backward pump-to-forward pump ratios ($I_b/I_f \geq 10$), accounting for reflection losses, we note that over 90% of the power in the backward pumpe beam was observed to be diffracted in the direction of the PCR

output. With the use of anti-reflection coated optics, and an external gain medium and feedback path, it should be possible to demonstrate a self-pumped PCR in this basic configuration. One such scheme is shown in Figure 3, where mirrors M4 and M5 are used to start up the oscillation of the 'normal' laser around the gain medium, and are then removed rapidly, i.e. faster than the $BaTiO_3$ PCR response times, to obtain a realization of a self-pumped PCR. Note that in this configuration the PCR is essentially the same linear PCR as in Figure 1, with perhaps the addition of an intracavity aperture for transverse mode control; the rest of the optics and the gain medium are principally for regeneration of the pumps, their power distribution and redirection. Clearly, several other arrangements and simplifications of this configuration appear possible.

In conclusion, we have reported new data on the spatial and temporal properties of a PCR based on the photorefractive crystal $BaTiO_3$, for the cases of single longitudinal mode and multi-longitudinal mode pumping. The highly anisotropic photorefractive effect has been observed to result in an elongated transverse mode in such a resonator for the case of single longitudinal mode pumping, and poor spatial quality and extremely long buildup times have been observed for multi-longitudinal mode pumping. A configuration is described that should permit self-pumped laser action in such a resonator.

We acknowledge the generous advice of R. Buchanan on the poling of $BaTiO_3$, and several very useful conversations with J. Feinberg and J. O. White on their experience with poling and beam coupling experiments. The generous assistance of D. G. Steel and R. A. McFarlane, and numerous conversations with G. C. Valley, M. B. Klein, and R. C. Lind are also gratefully acknowledged. This work was supported by AFOSR Contract #F49620-80-C-0041.

References

1. J. Feinberg and R. W. Hellwarth, Opt. Lett. 5, 519 (1980); erratum: Opt. Lett. 6, 257 (1981).
2. R. C. Lind and D. G. Steel, Opt. Lett. 6, 554 (1981).
3. J. O. White, M. Cronin-Golomb, B. Fischer, and A. Yariv, Appl. Phys. Lett. 40, 450 (1982).
4. V. V. Voronov, I. R. Dorosh, Yu. S. Kuzminov and N. V. Tkachenko, Sov. J. Quant. Electron. 10, 1346 (1980).
5. I. R. Dorosh, Yu. S. Kuzminov, N. M. Polozkhov, A. M. Prokhorov, V. V. Osiko, N. V. Tkachenko, V. V. Voronov, and D. Kh. Nurligareev, Phys. Stat. Sol. (a) 65, 513 (1981).
6. J. Feinberg, J. Opt. Soc. Am. 72, 46 (1982).
7. Our own observations, unpublished.
8. Electric fields of ~1.11 KV/mm were applied for a few hours at a temperature of ~145°C (~15°C above the Curie temperature); details of this technique were kindly provided to us by R. Buchanan, Univ. of Illinois.
9. I. Camlibel, M. DiDomenico, Jr., and S. H. Wemple, J. Phys. Chem. Solids 31, 1417 (1970).
10. This varies typically from 30 to 90%, depending clearly on the size of the aperture; similar beam elongation and power reduction with the use of intracavity apertures has also recently been observed by P. Günter, private communication.
11. V. L. Vinetskii, N. V. Kukhtarev, S. G. Odoulov, and M. S. Soskin, Sov. Phys. Uspekhi 22, 742 (1979).
12. B. Fischer, M. Cronin-Golomb, J. O. White, and A. Yariv, Opt. Lett. 6, 519 (1981).

Figure Captions

Figure 1 (a) Schematic of the basic experimental layout. The dashed lines represent optical elements that are inserted only for some of the experiments (see text).

(b) Details of the angular orientation of the $BaTiO_3$ crystals and input beams. The arrow marked c designates the direction and polarity of the crystal axis.

Figure 2: Far field photographs (a), (c), (e) and corresponding intensity profiles (b), (d), (f) of the output beam from the PCR. The intensity profiles correspond to the location of the cursor in the far field photographs. (a), (b): No intracavity aberrator. (c), (d): With intracavity aberrator. (e), (f): Characterization of the aberrator with a double pass transit of the probe beam.

Figure 3: One possible configuration for a self-pumped phase conjugate resonator. M4 and M5 represent removable mirrors that are only used for the "start-up" of this self-pumped PCR; the long memory times of $BaTiO_3$ facilitate the removal of these mirrors to obtain final "self-pumped" operation.

11797-1

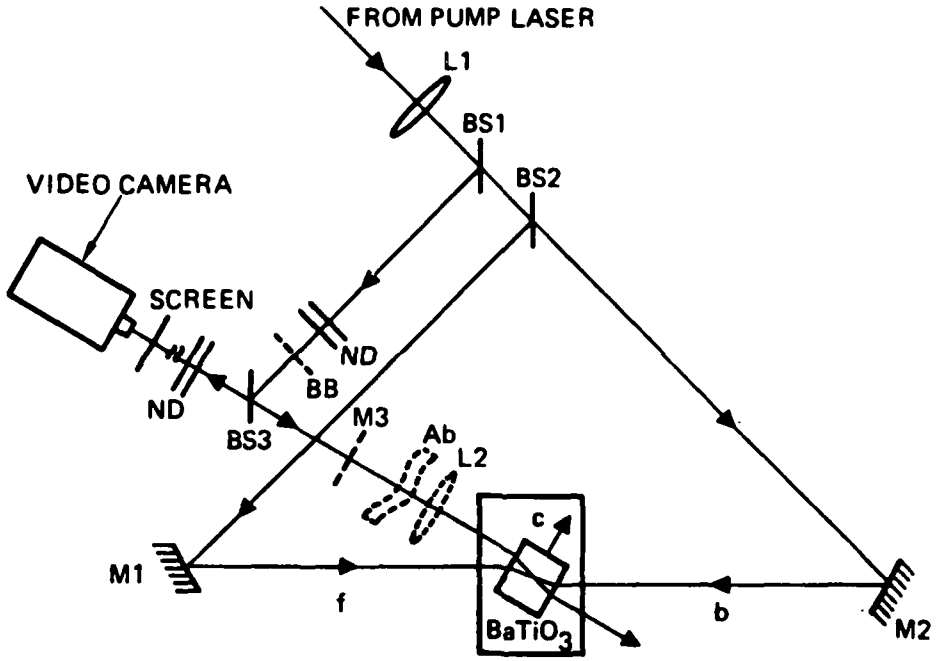

Fig.1(a)

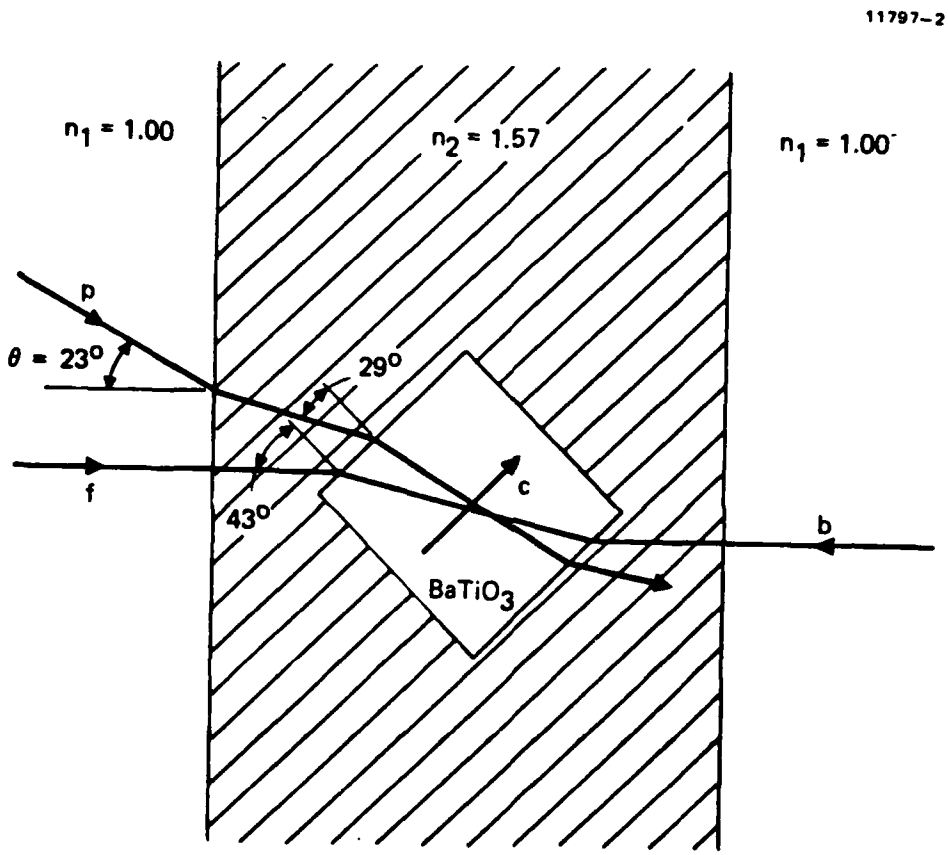

Fig.1(b)

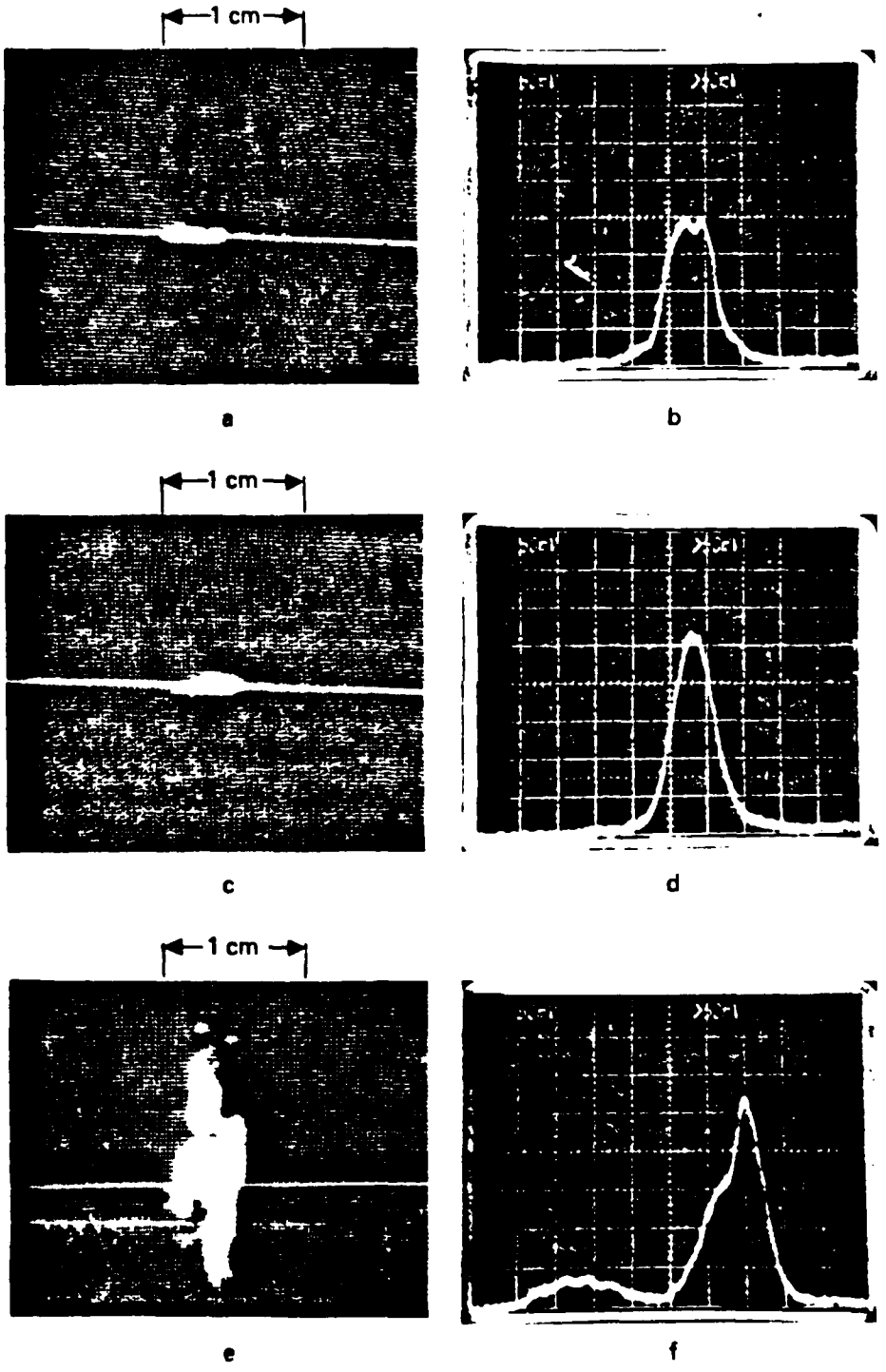

Fig. 2

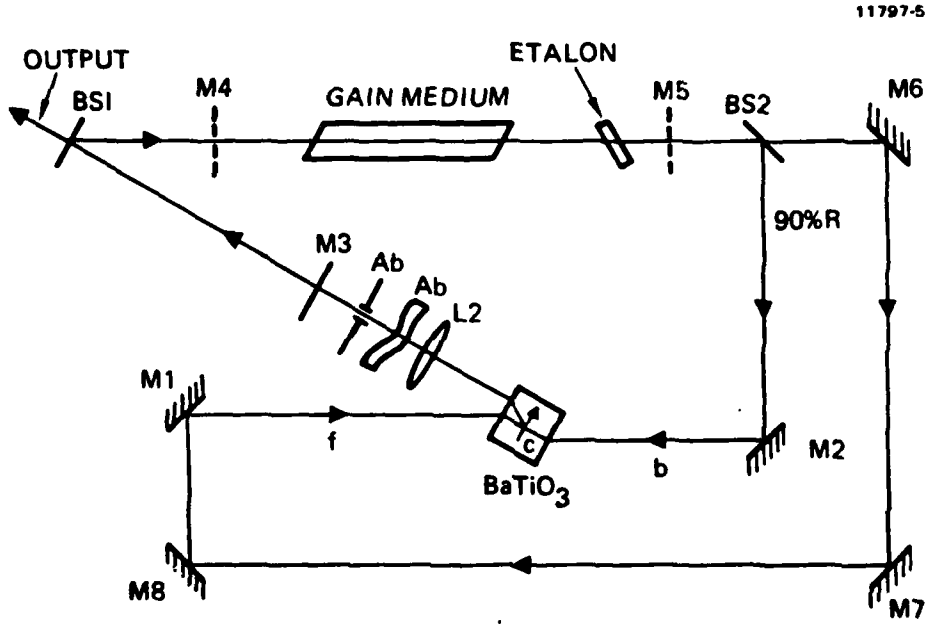
11797-5
OUTPUT
BSI
M4
GAIN MEDIUM
ETALON
M5
BS2
M6
90%R
M3
Ab
Ab
L2
M1
f
c
b
M2
BaTiO3
M8
M7

Fig. 3

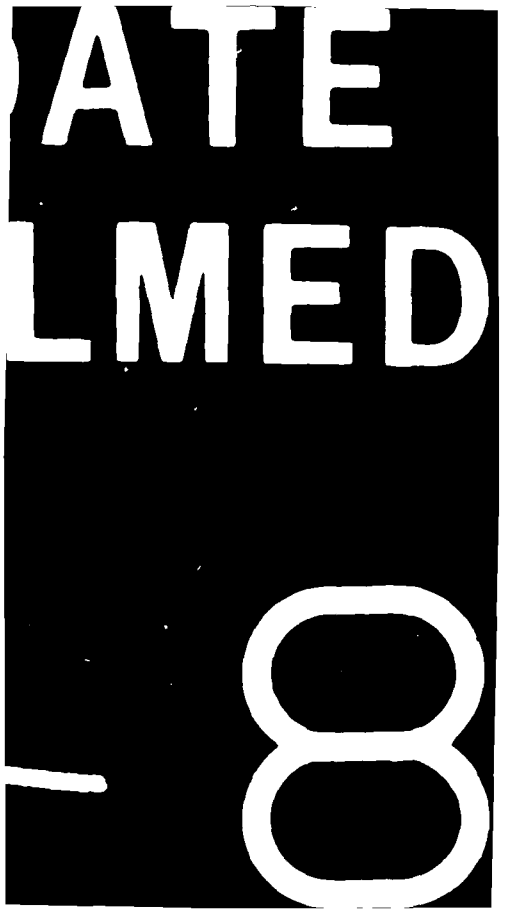
ATE
LMED
8